

ADVANCED OPTICAL MATERIALS

Supporting Information

for *Advanced Optical Materials*, DOI: 10.1002/adom.201700178

Ultrastrong Terahertz Emission from InN Nanopyramids on
Single Crystal ZnO Substrates

Huiqiang Liu, Zuxin Chen, Sheng Chu, Xuechen Chen, Min
Liu, Nan Peng, Guang Chu, Feng Huang, and Rufang Peng*

((Supporting Information can be included here using this template))

Copyright WILEY-VCH Verlag GmbH & Co. KGaA, 69469 Weinheim, Germany, 2017.

Supporting Information

Ultra-strong terahertz emission from InN nanopylamids on single crystal ZnO substrates

Huiqiang Liu[†], Zuxin Chen[†], Sheng Chu^{}, Xuechen Chen, Min Liu, Nan Peng, Guang Chu, Feng Huang, and Rufang Peng*

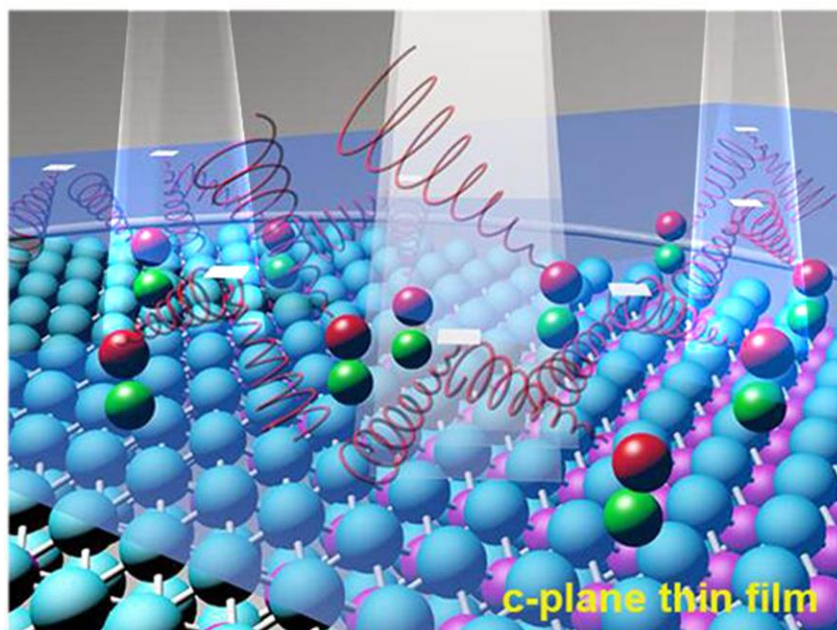


Fig. S1. Illustration of a thin film THz emitter. Due to the angular dependence of radiation by oscillating dipoles, as marked by white arrows, most of the produced THz waves bounce back into the film, causing a significant reflection loss.

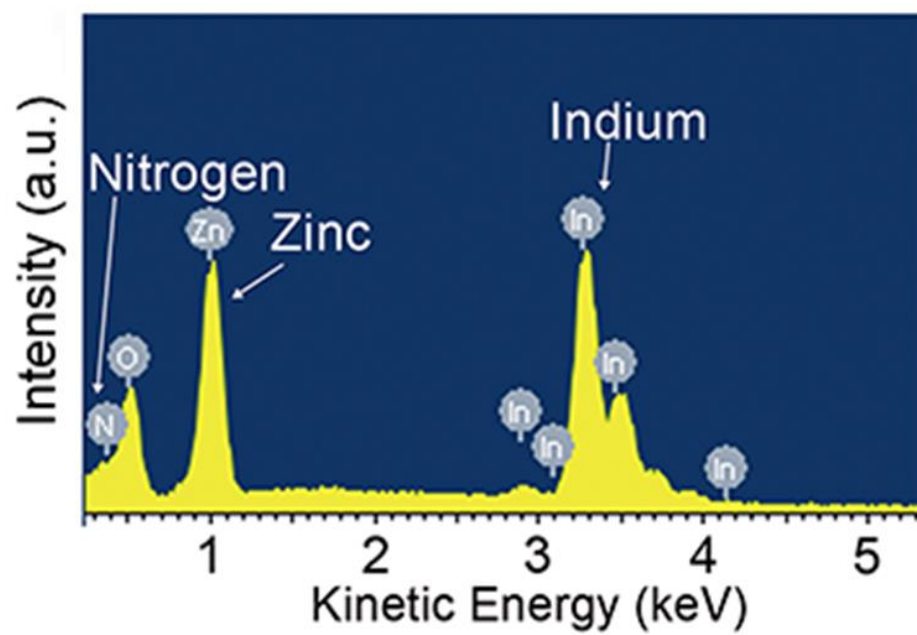


Fig. S2. EDS spectrum of the InN nanopyramids on ZnO.

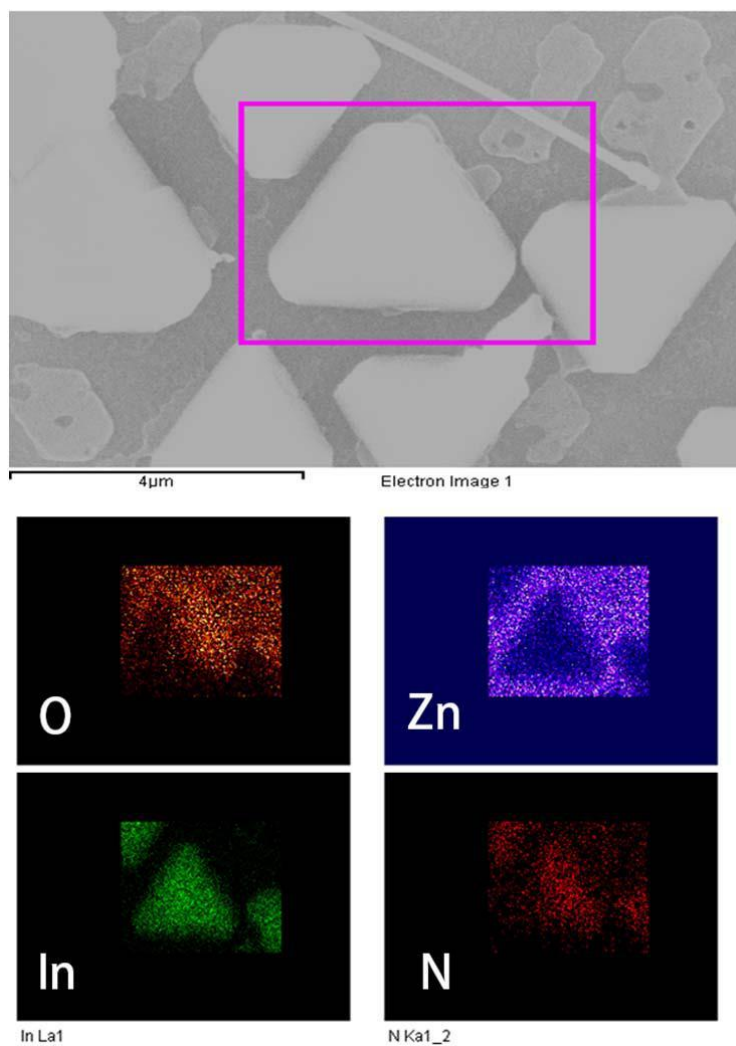


Fig. S3. EDS mappings on the InN nanopyramid/ZnO samples. Evidently, the In and N elements are on the nanopyramid region, while Zn and O are on the substrates.

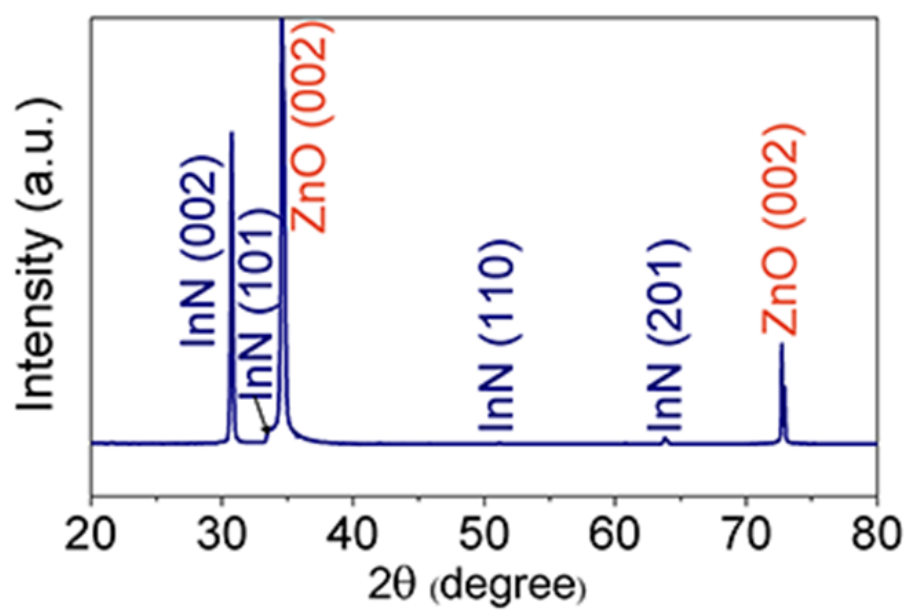


Fig. S4. θ - 2θ XRD scanning of the InN nanopyramids on ZnO.

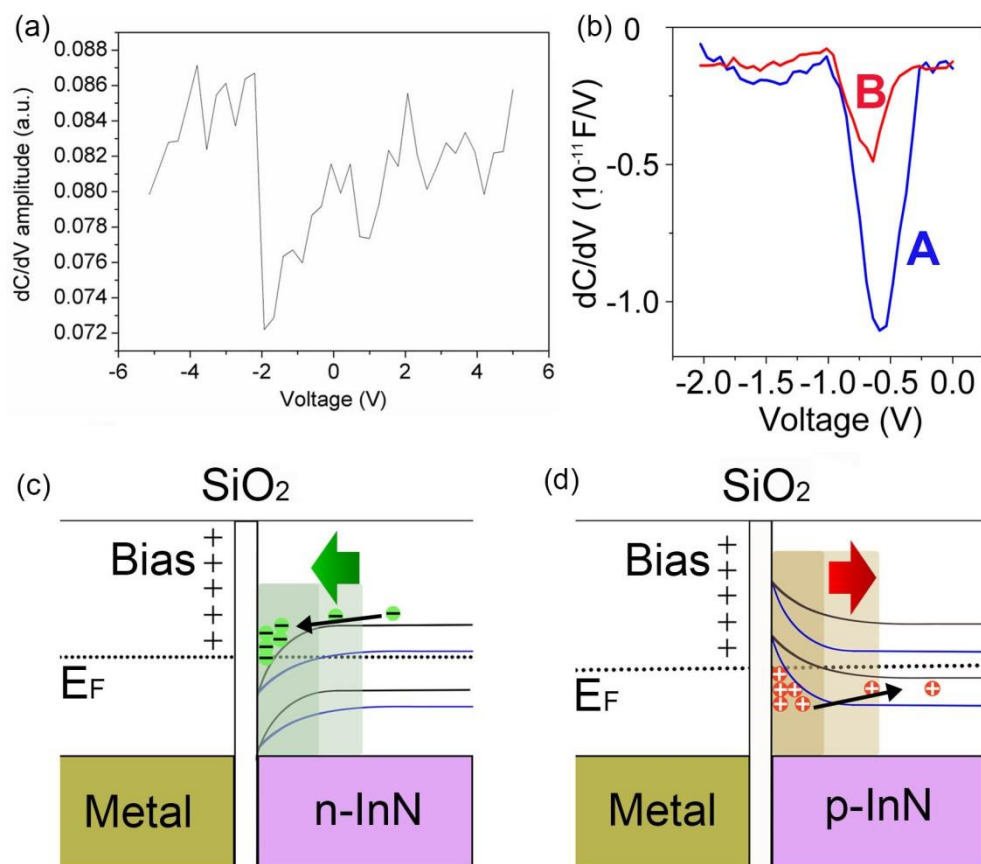


Fig. S5. (a) Typical dC/dV plot on the sample without SiO_2 deposition. The InN and InN/ZnO do not display junction-like C-V feature, which is possibly due to inhomogeneous Zn doping. In this case, many InN regions are not p-type which shorten the p-n junction region and show non-change C-V curve. (b) Plots of dC/dV vs bias for points A and B. (c) Schematic of the C-V measurement on p-type semiconductor. With an increase of bias, the depletion region increases while capacitance decreases. (d) Schematic of the C-V measurement on n-type semiconductor. With an increase of bias, the depletion region decreases while capacitance increases. In the SCM experiment, firstly, a metallized tip is used to form a local metal-insulator-semiconductor (MIS) structure where the contact is formed between the native oxide on the tip and the semiconductor; Secondly, the local MIS capacitance (or even better the capacitance variation) dependence of a small AC bias voltage ($f \sim 50$ kHz) is measured via a high-frequency circuit which applied the classical theory of MIS structures and their C-V curves. Since the C-V curve of n- and p-type samples is qualitatively inverted at the voltage axis, the sign of the ratio C/V directly reveals the type of majority carriers (electrons or holes).

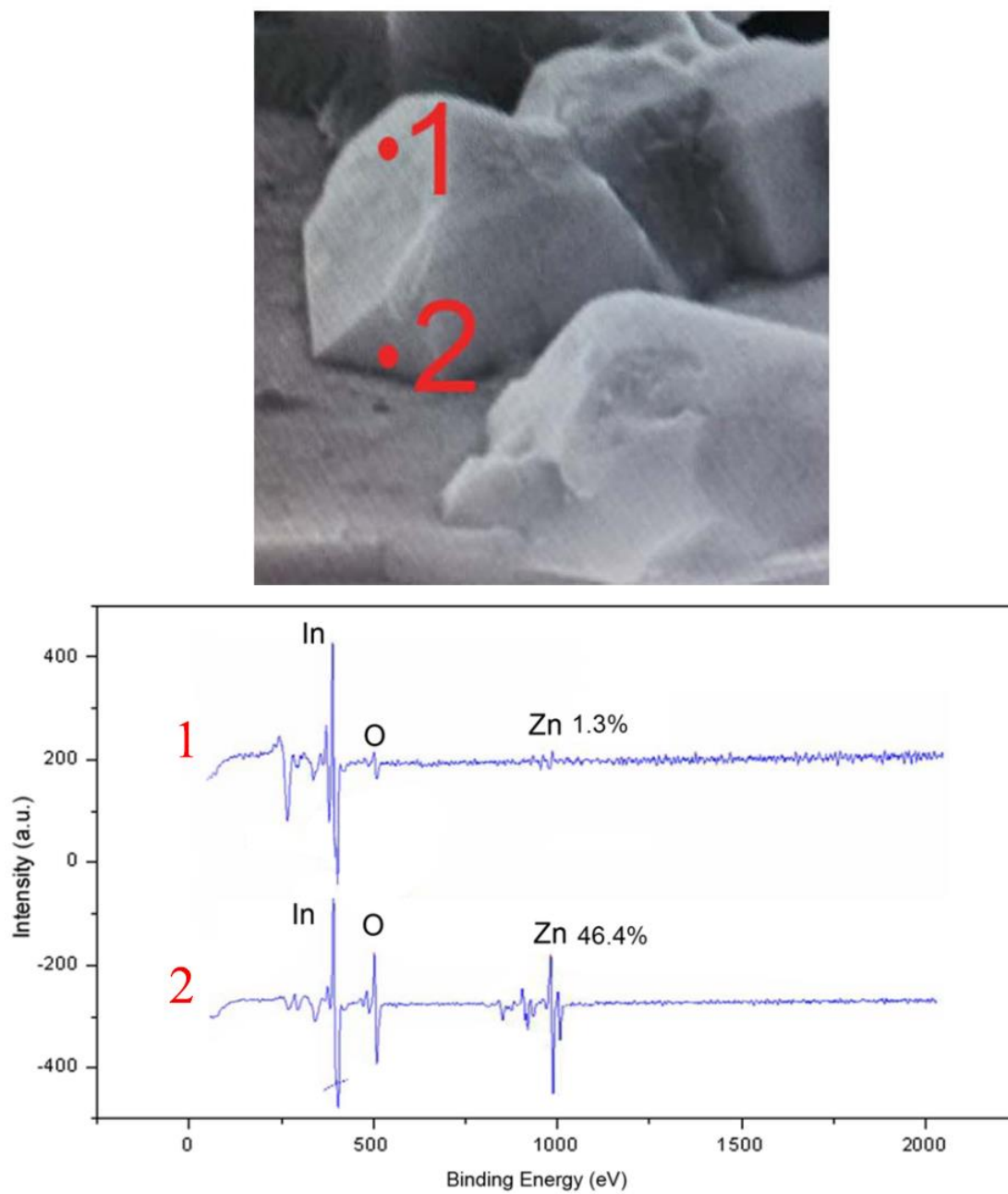


Fig. S6. The Auger spectra for representative points 1 and 2.

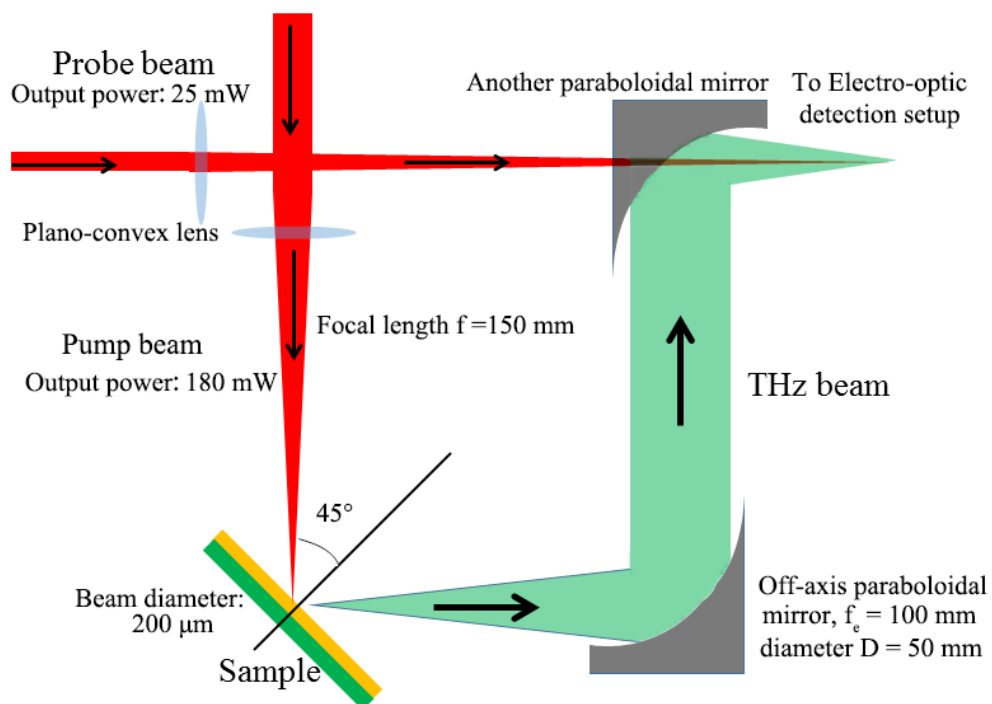


Fig. S7. Schematic experimental setup of the THz waveform generated from p-InAs (hole concentration of $3 \times 10^{16} \text{ cm}^{-3}$), p-GaAs (hole concentration of $1 \times 10^{16} \text{ cm}^{-3}$), and InN/ZnO samples with $90 \mu\text{J}/\text{cm}^2$ excitation density, respectively.

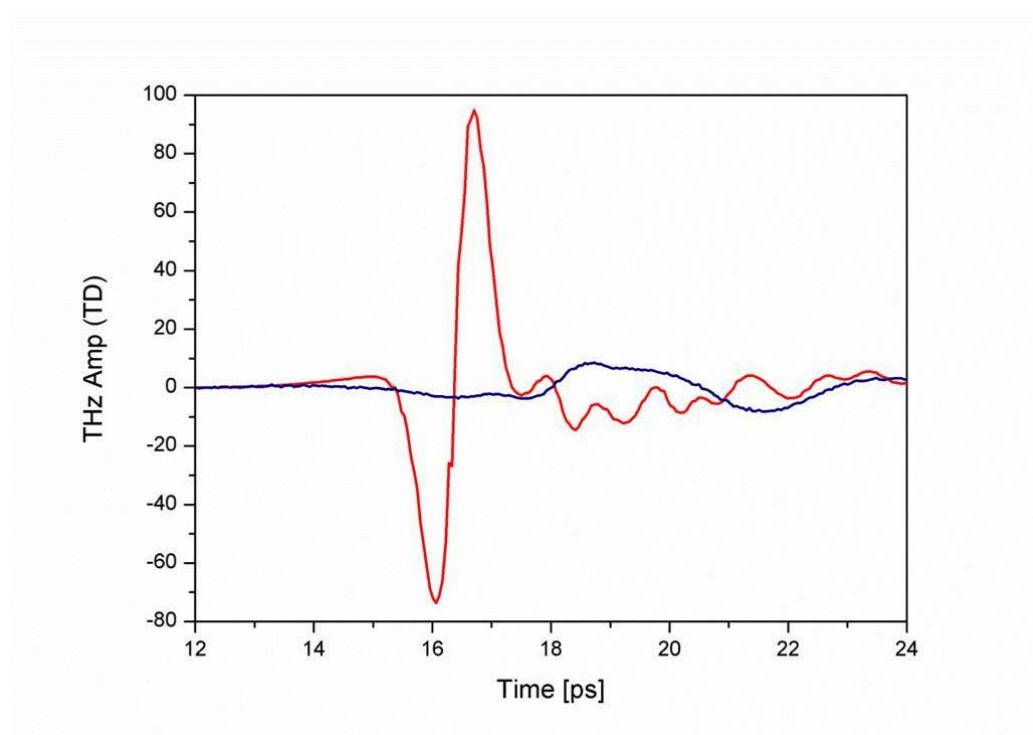


Fig. S8. Time resolved waveform for InN/ZnO sample (red) and bare ZnO substrate (blue).

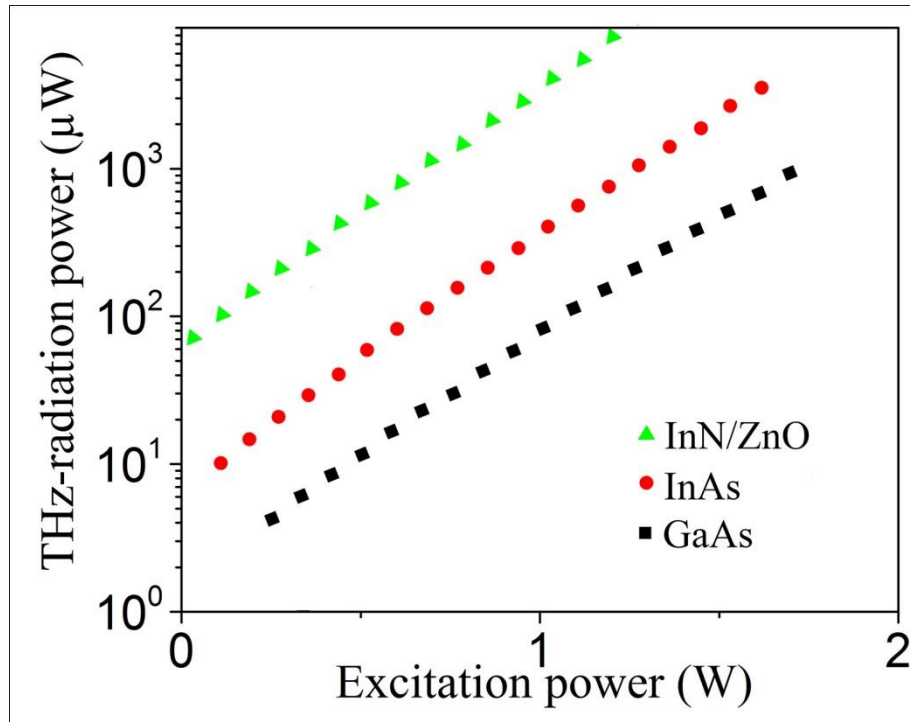


Fig. S9. Time-Excitation-power dependence of THz-radiation power.